Graphical Technique for Analyzing Marginally Stable Dynamic Systems

MARTEN T. LANDAHL*
McDonnell Aircraft Corporation, St. Louis, Mo.

It is shown how important qualitative and quantitative information on the dynamic stability characteristics of a linear system can be extracted rather easily from the Argand diagram of the characteristic equation for sinusoidal motion. This diagram reveals directly whether the system possesses marginally stable eigenvalues and also if violent instability may occur for a system with fluid flow (e.g., flutter). In addition, accurate estimates of marginally stable eigenvalues, including amplification or decay rates, may be obtained from the diagram. The method is applied to a model problem of membrane flutter which previously has been employed in a problem of boundary-layer stability. This model exhibits three essentially different classes of instability which are believed to be basic to all problems involving flowing fluids. Some simple cases of flutter are also considered which demonstrate the practical usefulness of the method and its accuracy.

Nomenclature

a	= speed of sound
b	= semichord of wing
d	= damping coefficient for membrane
$E(\lambda)$	= analytic expression of characteristic equation
g	= structural damping coefficient
k	= wave number for membrane deformation
$L_1, L_2, \ldots L_6$	= dimensionless oscillatory lift coefficients
m	= mass per unit span or area
$M_1, M_2, \ldots M_6$	= dimensionless oscillatory moment coefficients
$N_1, N_2, \ldots N_6$	= dimensionless oscillatory hinge moment coefficient
r_α	= radius of gyration of wing section (referred to elastic axis)
r_β	= radius of gyration of aileron
T	= membrane tension per unit width
U	= freestream velocity
x_0	= nondimensional distance of elastic axis behind leading edge, referred to chord, $2b$
x_α	= nondimensional distance of c.g. location for wing + aileron behind elastic axis
x_β	= nondimensional distance of c.g. location for aileron behind hinge line
γ	= exponential decay rate
δ	= $kd/\rho\omega_0$, nondimensional damping coefficient for membrane
μ	= mass density ratio; for wing section, $\mu = m/4\rho b^2$; for membrane, $\mu = mk/\rho$
λ	= $\omega + i\gamma$
ρ	= density of fluid
ω	= frequency of oscillation
ω_0	= $k(T/m)^{1/2}$, natural frequency of membrane
ω_h	= uncoupled natural bending frequency
ω_α	= uncoupled natural torsion frequency
ω_β	= uncoupled natural aileron frequency

Introduction

IN the stability analysis of a linear dynamic system with constant coefficients, the most difficult practical problem is usually to find the roots $\lambda = \lambda_n$ of the characteristic equation for the system

$$E(\lambda) = 0 \tag{1}$$

which determine whether harmonic motion of the form $Re[\exp(i\lambda t)]$ is possible without external excitation.† Here $\lambda = \omega + i\gamma$, where ω is the frequency and γ the exponential decay rate. For many cases of engineering interest, the expression for E is often so complicated that a complete analytic solution is not possible. In particular, E may be transcendental, which is frequently the case for systems involving fluid flow (for example, in flutter and in shear flow stability problems). Because of the great difficulty in solving Eq. (1), the analysis is usually limited to finding the stability boundary of the system, i.e., the combination of system parameters for which the system is neutrally stable. Some simple physical reasoning is then employed to determine on what side of the stability boundary instability occurs.

In the case of flutter, the restriction to purely real eigenvalues thus allows the use of aerodynamic forces calculated for purely harmonic motion. In general, since the characteristic equation is complex, each real value $\lambda = \omega$ specifies a pair of system parameters. It is convenient in flutter problems to choose one of these parameters to be the velocity (made suitably dimensionless) and the other to be, for example, the density ratio or any other suitable parameter for altitude. In an alternate, presently widely accepted method, the so-called U-g method, one chooses for the second parameter the fictitious structural damping g that is required to sustain neutrally stable oscillations for a given set of structural and flight parameters. Whenever, for some velocity $U = U_F$, the fictitious damping becomes equal to the actual internal damping of the structure, undamped oscillation, i.e., flutter, is possible. One usually displays the results in the form of a diagram of U vs g on the implicit assumption that the shape of the U-g curve reveals something about the severity of flutter for speeds beyond the flutter speed. Such interpretation must be made with great caution, however, lest completely erroneous conclusions be drawn. Investigations by Zisfein and Frueh[1-3] demonstrate that the amplification rate for unstable oscillations is related to the required damping through an expression involving the rate of change of flutter frequency with velocity; thus there is no direct one-to-one relationship between amplification rate and structural damping.

In automatic control engineering, the most widely used method to determine whether or not a system is stable is the

Presented as Preprint 64-83 at the AIAA Aerospace Sciences Meeting, New York, January 20–22, 1964; revision received June 3, 1964.

* Consultant; also, Professor of Aeronautics and Astronautics, Massachusetts Institute of Technology, Cambridge, Mass. Member AIAA.

† In problems with fluid flow it has been found more convenient and instructive to write the time-dependence this way, rather than as $\exp(st)$, which is common in control engineering terminology.

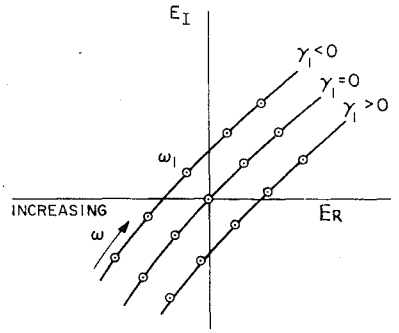

Fig. 1 Behavior of characteristic curve near a simple, almost real, root.

Nyquist criterion. This graphical technique is quite simple and could in principle also be used for problems involving fluid flow as in flutter (see Dugundji[4]). However, it presupposes among other things a knowledge of the behavior of the system for large complex frequencies which in problems with flow is difficult to determine. Also, it does not give any information regarding the actual eigenvalues, or even the degree of instability or stability.

It is obvious that information on true complex eigenvalues $\lambda_n = \omega_n + i\gamma_n$ for other combinations of system parameters than those corresponding to neutrally stable cases would be extremely useful, in particular for small decay rates γ_n. Not only would one then be able to judge the severity of an instability but also the degree of stability, which is of importance in calculating the response to a disturbance. In addition, one could then calculate the eigenmodes that are of interest, for example, when trying to find the most efficient cure for an instability.

It is the purpose of the present paper to point out that many of the stability properties of interest may be read rather directly from what will here be called the characteristic diagram. This is an Argand diagram of the characteristic equation plotted for real frequencies $\lambda = \omega$. (The modified Nyquist diagram is such a one.) From the characteristic diagram one can also easily estimate with good accuracy those eigenvalues which are close to the real axis. This method, originally suggested in Ref. 5, has been found to be a useful complement to computer-based stability calculations for complicated systems involving fluid flow, since it furnishes with comparatively little effort a visual aid for the

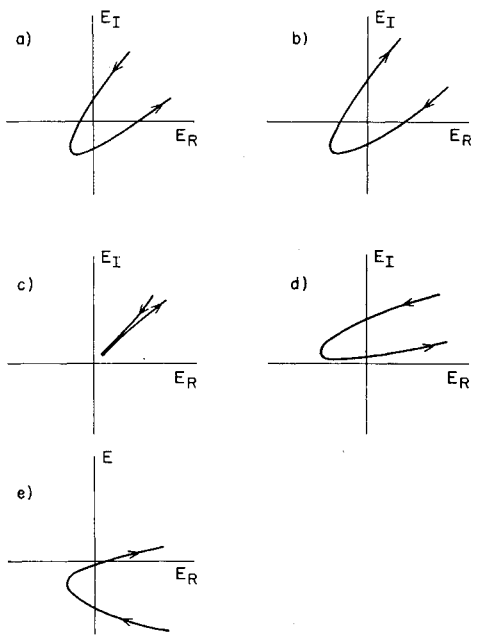

Fig. 2 Two clustered roots: a) both roots stable, b) both roots unstable, c) complex conjugate roots, d) unstable root closer to real axis, and e) stable root closer to real axis.

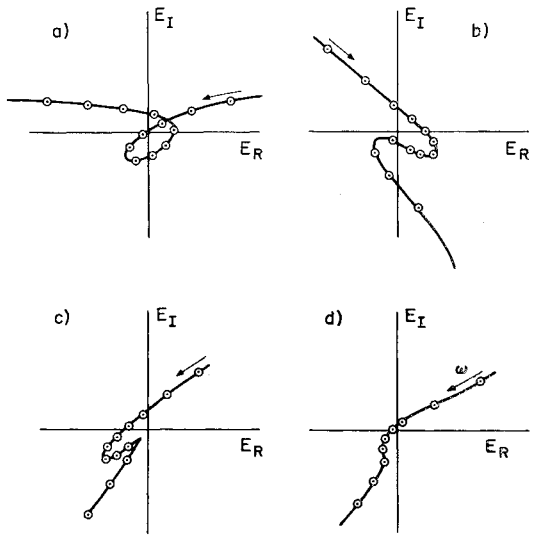

Fig. 3 Three clustered roots: a) one neutrally stable, two stable; b) two unstable, one stable; c) one stable, two (nearly) complex conjugates; and d) two stable, one unstable.

understanding of the stability characteristics. In addition, it provides a good first estimate of the most important eigenvalues to use as starting values in an iteration scheme.

Properties of the Characteristic Diagram Near Almost Real Roots

It will be assumed from the outset that the characteristic equation (1) has no poles near the real axis, or at least that the poles are all well removed from the zeros. If not, the equation can be easily modified so that the poles are removed (see Ref. 5). Otherwise it is rather unimportant what form the characteristic equation takes or how it was obtained. $E(\omega)$ could, for example, represent the (complex) impedance experienced by an oscillator applied to any point of the system, i.e., it could be determined experimentally. The characteristic diagram is obtained by plotting the imaginary part E_I vs the real part E_R with ω as a parameter.

We will first study the behavior of the characteristic curve in the neighborhood of an almost purely real eigenvalue $\lambda = \lambda_1 \equiv \omega_1 + i\gamma_1$ for the case when this root is well separated from other roots. In the neighborhood of the root, E would behave like

$$E(\lambda) = (\lambda - \lambda_1)P(\lambda) \tag{2}$$

where P can be assumed to vary so slowly that it may be considered a constant in a small region around λ_1. Alternatively, we may consider (2) as the first term in a Taylor-series expansion around λ_1 so that

$$P(\lambda_1) = (dE/d\lambda)_{\lambda=\lambda_1} \tag{3}$$

Under this assumption $E(\omega)$ will behave in the same manner as $\omega - \lambda_1$. Hence, the curve will pass through the origin only if λ_1 is purely real. For $\gamma_1 > 0$, i.e., for a stable root, $\omega - \lambda_1$, and thus E, will rotate an angle $+\pi$ as $\omega = \omega_1$ is passed. In the case of $\gamma_1 < 0$, on the other hand, it will rotate an angle of $-\pi$. The three cases are illustrated in Fig. 1. A stable or unstable root will thus be indicated, depending on whether the characteristic curve passes to the right or to the left of the origin, a rule that is sometimes used in control engineering.

This rule will fail when there are two or more roots located close together. Consider first the case of two closely spaced roots. In the neighborhood of these, the characteristic equation behaves like

$$E = (\lambda - \lambda_1)(\lambda - \lambda_2)Q(\lambda) \tag{4}$$

where Q is a slowly varying function that may be assumed constant in a small region around λ_1 and λ_2. If λ_1 and λ_2 are complex conjugates, or nearly so, the function E may not rotate as λ_1 or λ_2 is passed. However, this case may be analyzed by considering the derivative of E,

$$\frac{dE}{d\lambda} \simeq 2\left(\lambda - \frac{\lambda_1 + \lambda_2}{2}\right) Q(\lambda) \tag{5}$$

which will rotate an angle π or $-\pi$, depending on whether the stable or the unstable root is farther from the real axis. The various different cases that may occur are illustrated in Fig. 2.

When more than two roots are located close together, the identification of unstable roots becomes increasingly difficult. With three clustered roots the characteristic equation behaves like

$$E = (\lambda - \lambda_1)(\lambda - \lambda_2)(\lambda - \lambda_3)R(\lambda) \tag{6}$$

where R is a slowly varying function. In this case, the Argand diagram of the first derivative

$$\frac{dE}{d\lambda} \simeq [3\lambda^2 - 2\lambda(\lambda_1 + \lambda_2 + \lambda_3) + \lambda_1\lambda_2 + \lambda_1\lambda_3 + \lambda_2\lambda_3]R \tag{7}$$

is a parabola with vertex for an ω near the three roots. Depending on the location of the vertex relative to the origin, the curve for E may or may not make a turn of an angle less than 2π. Since $|dE/d\lambda|$ will be minimum in the neighborhood of the three roots, the points for equidistant values of ω will cluster closest together in the region of the roots. Some possible (but not all) cases that may occur are illustrated in Fig. 3.

It would be quite difficult to analyze cases of more than three clustered roots. Fortunately, such cases are very rare in practice. In fact, even cases with three clustered roots seem to be fairly unusual.

Graphical Estimate of Nearly Real Eigenvalues

By making use of the analytical properties of the characteristic equation, one can obtain estimates of those eigenvalues that are located close to the real axis. We will first consider the case when the roots are well separated. As in (2), we may then assume that E can be approximated by a function linear in λ in some small neighborhood of the root λ_1 which includes, e.g., the point $\lambda = \omega_p$ (see Fig. 4).

The characteristic equation (1) then may be approximated by

$$E \simeq E(\omega_p) - (\lambda - \omega_p)(dE/d\lambda)_{\lambda=\omega_p} = 0 \tag{8}$$

Solving for the root $\lambda = \lambda_1$ we obtain

$$Z_1 \simeq \omega_p - [E/(dE/d\omega)]_{\lambda=\omega_p} \tag{9}$$

We can make the second term purely imaginary by selecting ω_p such that E is normal to $dE/d\omega$ at the point.‡ Thus, the real part of the eigenvalue ω_1 is obtained approximately as the frequency corresponding to which the normal from the origin intersects the characteristic curve. The exponential decay rate is then given by

$$\gamma_1 \simeq \pm(|E|/|dE/d\omega|)_{\omega=\omega_1} \tag{10}$$

where the sign is to be chosen as plus or minus, depending on whether the curve passes to the right or left of the origin. The quantities appearing in (10) may be obtained approximately from the diagram simply by measuring with a ruler. With the distances as defined in Fig. 4 (arbitrary units) we thus obtain

$$\gamma_1 \simeq (N/\Delta E)(\omega_q - \omega_p) \tag{11}$$

‡ Lines of constant ω and γ must be orthogonal, since $E(\lambda)$ is a conformal transformation.

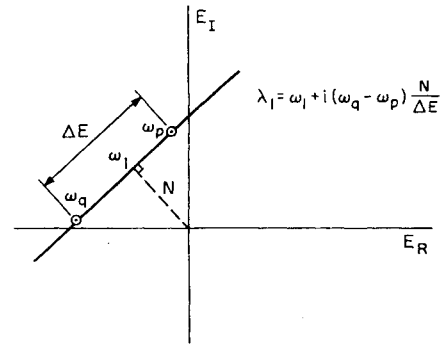

Fig. 4 First graphical method for estimating eigenvalues

which will be referred to as the first method.

This method will fail when several roots are located close together. A second method will therefore be developed which is applicable to the case of two clustered roots. In this case (4) applies in the neighborhood of the two roots, and the characteristic curve may thus be approximated by a parabola.

Without loss of generality, we may assume that the coordinate system is rotated such that the real axis is parallel to the axis of the parabola (see Fig. 5). Using the notation of Fig. 5 the characteristic curve is given by

$$E_R = K_1(\omega - \omega_v)^2 + R \tag{12}$$

$$E_I = K_2(\omega - \omega_v) + S \tag{13}$$

where K_1 and K_2 are constants that may be obtained from measured values of X and Y as follows:

$$K_1 = X/(\Delta\omega)^2 \tag{14}$$

$$K_2 = Y/(2\Delta\omega) \tag{15}$$

where $\Delta\omega = \omega_v - \omega_p = \omega_q - \omega_v$, and ω_v is the frequency for the vertex of the parabola. Employing analytic continuation we may thus approximate the characteristic equation by

$$E(\lambda) = K_1(\lambda - \omega_v)^2 + iK_2(\lambda - \omega_v) + R + iS \tag{16}$$

which possesses the two solutions

$$\lambda_{1,2} = \omega_v - \frac{iK_2}{2K_1} \pm i\left(\frac{R + iS}{K_1} + \frac{K_2^2}{4K_1^2}\right)^{1/2} \tag{17}$$

This result is somewhat more complicated than the earlier one [Eq. (11)], since it involves calculating the square root of a complex number.

Classification of Instabilities for Systems Involving Fluid Flow

As the first application we will consider the instability of an infinite membrane in an incompressible and inviscid flow.

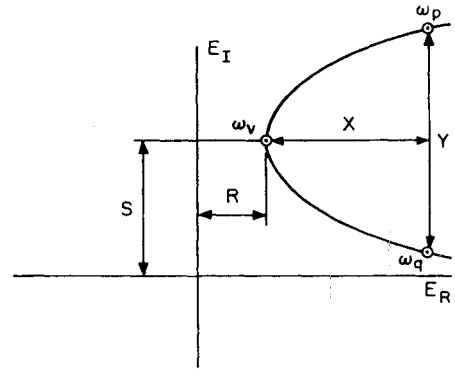

Fig. 5 Second graphical method.

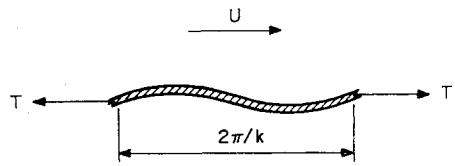

Fig. 6 Membrane flutter problem.

This simple case is extremely instructive and may serve as a simplified model for both panel flutter and boundary-layer instability. It also incorporates what is believed to be all the essential stability properties of systems with fluid flow. The model has been discussed in great detail by Landahl[5] and by Benjamin,[7] and we will therefore emphasize only those aspects that pertain to the present graphical technique.

The motion of a stretched membrane of mass m per unit area, tension T per unit span, and damping coefficient d is governed by the equation

$$Ty_{xx} - my_{tt} - dy_t = p \tag{18}$$

where $y(x, t)$ is the deformation of the membrane and $p(x, t)$ the pressure applied, which in the present case is that induced by the flow due to the membrane deformation. The balance of the two sides of Eq. (18) indicates when self-sustained motion is possible. For an infinite membrane, the appropriate eigenfunction is an infinite (traveling) wave of the form

$$y = \hat{y} \exp[i(\lambda t - kx)] \tag{19}$$

where $\hat{y}$ is a constant and k is the wave number (see Fig. 6). This deformation can easily be shown to induce the following pressure in an incompressible, inviscid flow:

$$p = -\rho\hat{y}(U - \lambda/k)^2 \exp[i(\lambda t - kx)] \tag{20}$$

where ρ and U are the density and velocity, respectively, of the stream. The natural length scale in the present problem is the wave length $2\pi/k$ so that, by introducing the following dimensionless variables

$$\begin{aligned} \mu &= mk/\rho \\ \bar{U} &= Uk/\omega_0 \\ \bar{\lambda} &= \lambda/\omega_0 \\ \delta &= kd/\rho\omega_0 \end{aligned} \tag{21}$$

where

$$\omega_0 = k(T/m)^{1/2} \tag{22}$$

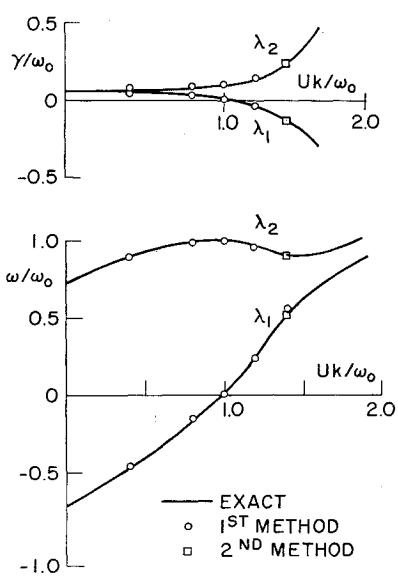

Fig. 7 Eigenvalues for membrane.

we obtain, after some manipulation, the following characteristic equation:

$$E \equiv \bar{\lambda}^2(1 + \mu) - \bar{\lambda}(2\bar{U} + i\delta) + \bar{U}^2 - \mu = 0 \tag{23}$$

The roots of this are given by

$$\bar{\lambda}_{1,2} = \frac{\bar{U} + i\delta/2}{1 + \mu} \pm \frac{[\mu(1 + \mu - \bar{U}^2) - \delta^2/4 + i\delta\bar{U}]^{1/2}}{1 + \mu} \tag{24}$$

In the numerical example chosen the following values were selected: $\mu = 1.0$ and $\delta = 0.2$. The real and imaginary parts of the eigenvalues are plotted vs the nondimensional velocity $\bar{U}$ in Fig. 7 and some of the associated characteristic diagrams in Fig. 8. Values obtained by the graphical methods given in the preceding section are also shown. The eigenvalues were obtained by the first method for $\bar{U} < 1.4$ and by the second method for $\bar{U} \geq 1.4$. As seen, the agreement between the exact and approximate values is very good.

There are several interesting properties that become apparent from the results. First, the root λ_1 goes unstable for $\bar{U} > 1$. This instability is clearly caused by the damping in the membrane, since it is easily seen from (24) that for $\delta = 0$ only neutrally stable roots are possible for $\bar{U} \leqq [\mu(1 + \mu)]^{1/2} = 2^{1/2}$. The physical explanation why damping may cause instability was given by Landahl[5] and further discussed by Benjamin.[7] For this class of instability, denoted by class A (Benjamin[6]), the total kinetic and elastic energy of the system (consisting of the membrane plus the fluid) is lower in the excited state than in the unexcited one. Therefore, removal of mechanical energy from the system through dissipation will cause the amplitude to grow in order to compensate for the energy loss.

The second root, on the other hand, is obviously stabilized by the damping for all velocities. In this class B type of wave (Benjamin,[6, 7] Landahl[5]), the energy perturbation of the system is positive, and dissipation thus acts to decrease the wave amplitude, hence aiding stabilization.

At higher velocities, the first root develops into an essentially third type of instability, a class C instability, which is characterized by a high amplification rate. In contrast to the other two, this instability is very little influenced by dissipation in the system. It was shown[5] that for a class C instability the total energy of the system stays essentially constant, and there is only a redistribution of energy between various parts of the system. With zero damping, class C instability will in the present example occur for $\bar{U} \geq [\mu(1 + \mu)]^{1/2} = 2^{1/2}$, in which case two complex conjugate roots will appear. In the characteristic diagram (Fig. 8), class C instability is indicated when the curve for E turns back without reaching the origin, as is the case for the curve for $\bar{U} = 1.6$. This class is not quite so distinct as the other two; it occurs in pure form only for zero damping, in which case the curve will double back onto itself along the real axis.

These three classes can be distinguished in a variety of problems. The most commonly occurring is the class B type; the majority of single- or multidegree flutter cases are of this type, as well as the generation of water waves by wind. For higher velocities, it usually carries over into a class C

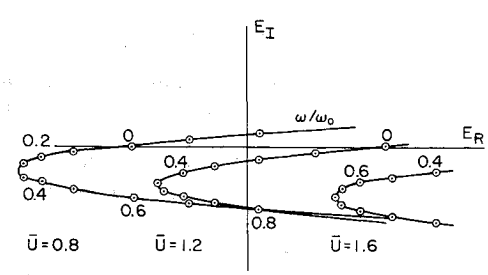

Fig. 8 Characteristic diagrams for membrane: $\mu = 1, \delta = 0.2$.

instability. In a lightly damped or undamped system, this class is associated with the familiar merging, or near merging, of two natural frequencies. Kelvin-Helmholtz instability is the archtype of class C instability. Since it is associated with a loss of resultant stiffness[5] rather than loss of damping, it is generally a dangerous instability of an explosive type which would generally lead to a complete breakup of any structure. In hydrodynamic stability, the instability of a free shear layer is mainly of this type, as well as the turbulent spots or bursts that appear in the final stage of the transition of a laminar boundary layer to turbulence.[8] The primary instability waves in a boundary layer, the Tollmien-Schlichting waves, are of the class A variety. This class also occurs in panel flutter and occasionally, as will be seen in an example to follow, in ordinary bending-torsion flutter.

Application to the Flutter of a Wing Section

To demonstrate the use of the method for flutter, we will consider some simple cases of two- and three-degree-of-freedom flutter of a two-dimensional section. For simplicity in calculating the aerodynamic forces, a high supersonic Mach number has been assumed, so that piston theory applies (with zero airfoil thickness). Of course, the present method can be used together with any analytical, numerical, or experimental set of data giving the aerodynamic coefficients as functions of the reduced frequency.

The flutter analysis of a typical section having the three degrees of freedom of bending (subscript h), torsion α, and aileron rotation β, gives rise to the following flutter determinant[9]:

$$E(\lambda) \equiv \left(\frac{\lambda}{\omega_\alpha}\right)^6 \begin{vmatrix} A & B & C \\ D & E & F \\ G & H & I \end{vmatrix} = 0 \qquad (25)$$

where

$$\begin{aligned} A &= \mu[(\omega_\alpha/\lambda)^2 - 1] + L_1 + iL_2 \\ B &= -\mu x_\alpha + L_3 + iL_4 \\ C &= -\mu x_\beta + L_5 + iL_6 \\ D &= -\mu x_\alpha + M_1 + iM_2 \\ E &= \mu r_\alpha^2[(\omega_\alpha/\lambda)^2 - 1] + M_3 + iM_4 \\ F &= -\mu[r_\beta^2 + 2(x_1 - x_0)x_\beta] + M_5 + iM_6 \\ G &= -\mu x_\beta + N_1 + iN_2 \\ H &= -\mu[r_\beta^2 + 2(x_1 - x_0)x_\beta] + N_3 + iN_4 \\ I &= \mu r_\beta^2[(\omega_\beta/\lambda)^2 - 1] + N_5 + iN_6 \end{aligned} \qquad (26)$$

and the standard American notation has been used (see, e.g., Ref. 10). The factor $(\lambda/\omega_\alpha)^6$ has been added for convenience to cancel the multipole at $\lambda = 0$. Piston theory values of the aerodynamic coefficients $L_1, L_2 \ldots N_6$ have been given in Ref. 11.

The subcase of two-degrees-of-freedom bending-torsion flutter is obtained from

$$E(\lambda) \equiv (\lambda/\omega_\alpha)^4 \begin{vmatrix} A & B \\ D & E \end{vmatrix} = 0 \qquad (27)$$

Eigenvalues for this case have been calculated by Zisfein and Frueh.[1] One case considered by them was for the following set of parameters:

$$\begin{aligned} \mu &= m/4\rho b^2 = 50 \\ x_\alpha &= 0.2 \\ r_\alpha &= 0.5 \\ \omega_h/\omega_\alpha &= 0.4 \\ x_0 &= 0.4 \\ a/b\omega_\alpha &= 2.325 \end{aligned}$$

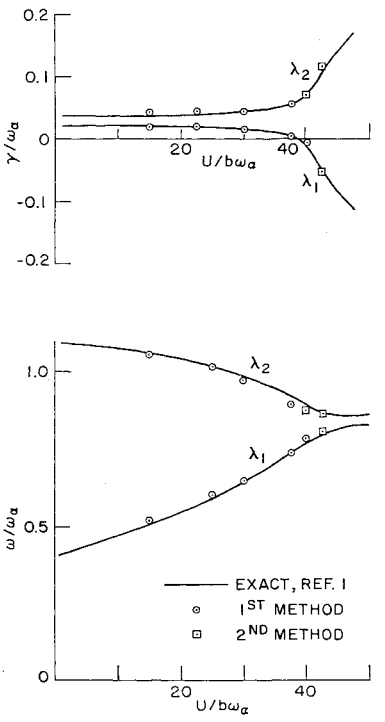

Fig. 9 Eigenvalues for bending-torsion flutter of zero-thickness wing section at high Mach numbers: $\mu = 50$, $x_\alpha = 0.2$, $r_\alpha = 0.5$, $\omega_h/\omega_\alpha = 0.4$, $x_0 = 0.4$, $a/b\omega_\alpha = 2.325$.

where a is the speed of sound. In Fig. 9 the graphical estimates of the eigenvalues for this system are shown as function of the reduced velocity $U/b\omega_\alpha$, together with the exact values from Ref. 1. As seen, the agreement is very good.

Some of the associated characteristic curves are shown in Fig. 10. These apparently resemble closely those for the membrane case considered in the preceding section with the lowest root going unstable. One would therefore suspect that the bending-torsion flutter in this case, as well, is of class A type. Introduction of structural damping by replacing ω_α^2 by $\omega_\alpha^2(1 + ig)$ and ω_h^2 by $\omega_h^2(1 + ig)$ gives the following characteristic equation:

$$E \equiv E(g = 0) + \Delta E = 0 \qquad (28)$$

where

$$\begin{aligned} \Delta E = i(\mu g/\omega_\alpha^2)\{\mu r_\alpha^2[2\omega_h^2 - \\ \lambda^2(1 + \omega_h^2/\omega_\alpha^2)] + \lambda^2[(\omega_h/\omega_\alpha)^2(M_3 + iM_4) + \\ r_\alpha^2(L_1 + iL_2)]\} \end{aligned} \qquad (29)$$

and terms of order g^2 have been neglected. In Fig. 11a the characteristic curves with $g = 0$ and $g = 0.05$ for $U/b\omega_\alpha =$

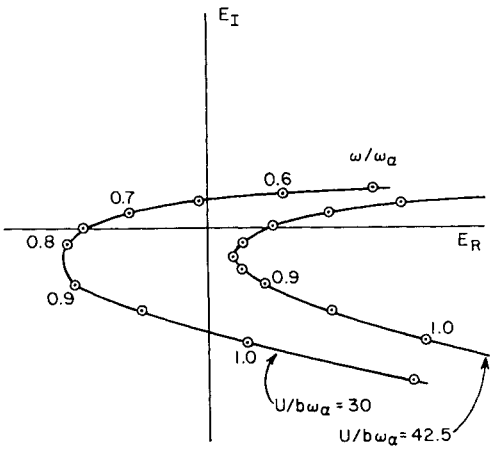

Fig. 10 Characteristic diagrams for the bending-torsion flutter case.

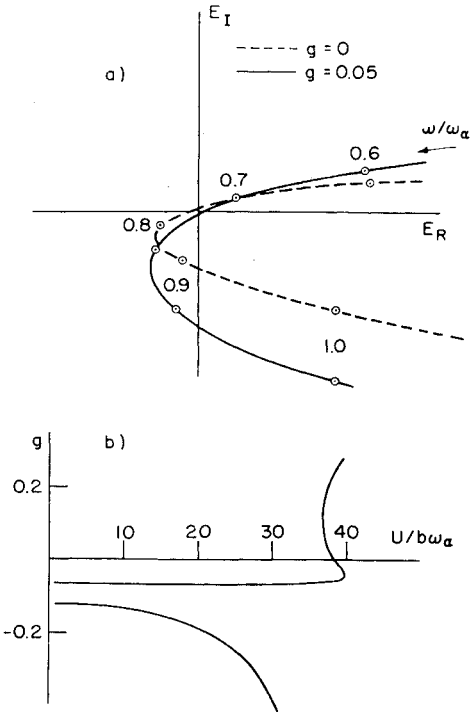

Fig. 11 Effect of structural damping on bending-torsion flutter: a) characteristic diagram for $U/b\omega_\alpha = 37.5$, and b) required structural damping to sustain neutrally stable oscillations.

37.5 are compared. It is seen that the damping will displace the curve downwards for $\omega/\omega_\alpha > \sim 0.7$ by a distance sufficient to cause instability. Particularly interesting in this case is the U-g curve of required damping for neutrally stable oscillations which is reproduced from Ref. 1. This curve exhibits a characteristic loopback that would always be typical of a class A instability since the destabilizing effect of damping must cause the flutter velocity to decrease.

Further examination of the calculations of Ref. 1 reveals the interesting fact that dissipation in form of viscous damping (instead of structural damping) does not have a destabilizing effect. With this type of damping, the characteristic curve is displaced upward instead of downward with stabilization as a result. The situation resembles to some extent that in boundary-layer stability in which viscosity may be either destabilizing or stabilizing depending on the Reynolds number. The study of the effect of the mode of damping on stability should be a fruitful one, since it might point the way toward effective ways of curing instability. With the present method, such a study would be comparatively simple. However, the possible increase in critical velocity attained by adding damping in a favorable manner would be limited, since once class C instability sets in, change of damping would be rather ineffective.

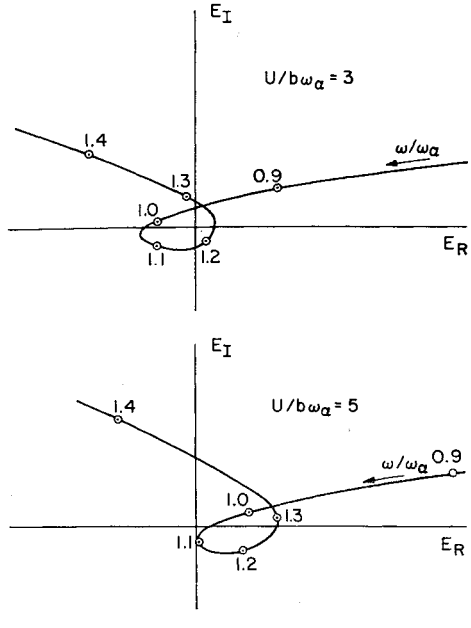

Fig. 12 Characteristic diagrams for bending-torsion-sileron flutter at high Mach numbers: $\mu = 50$, $x_\alpha = 0.2$, $r_\alpha = 0.5$, $\omega_h = \omega_\beta = \omega_\alpha$, $x_0 = 0.4$, $r_\beta = 0.1$, $x_1 = 0.8$.

A three-degree-of-freedom case for the following combination of parameters is also studied:

μ	$= 50$	$a/b\omega_\alpha$	$= 2.325$
x_α	$= 0.2$	x_β	$= 0$
r_α	$= 0.5$	r_β	$= 0.1$
ω_h/ω_α	$= 1.0$	$\omega_\beta/\omega_\alpha$	$= 1.0$
x_0	$= 0.4$	x_1	$= 0.8$

All the uncoupled frequencies were chosen equal in the expectation that this would cause the three eigenvalues to cluster close together for a severe test of the graphical technique. Two characteristic curves for velocities near the flutter velocity are shown in Fig. 12. More extensive calculations reveal that the lowest root goes unstable for $U/b\omega_\alpha \simeq 4.7$. Class C instability sets in very soon above this velocity. Since no published exact values are available for comparisons, graphical estimates of eigenvalues were not attempted in this case. However, because of the closeness of the three roots, less accuracy may be expected than in previous examples.

Conclusions

By making use of some elementary analytical properties to study the behavior of the characteristic diagram near almost real roots, graphical techniques were developed which proved useful essentially for two main purposes. First, the characteristic diagram was shown to reveal directly certain qualitative properties of the stability of the system, such as whether there are marginally stable roots, roots clustered together, or whether violent instability is about to occur. The threefold classification of instabilities which was originally proposed for the problem of stability of a laminar boundary layer over a flexible wall[5–7] is believed to be applicable for all systems involving fluid flow. Thus, for example, the violent class C instability will always occur if, for some mode of oscillation, the resultant effective dynamic stiffness becomes negative for all frequencies (because of the induced hydrodynamic forces). Class C instability may therefore be investigated approximately by neglecting aerodynamic and structural damping altogether, as was done by Zisfein and Frueh[1] in obtaining their so-called base curve for the eigenvalues.

The second purpose was to devise simple and completely general graphical techniques to estimate the marginally stable eigenvalues for complicated systems. Two methods were developed, one that approximated the characteristic curve by a straight line near the eigenvalue, and a second one that assumed the curve to be a parabola. The first method is the more useful because of its simplicity. It is similar to the damping-decay rate relationship discovered by Zisfein and Frueh[2,3] in that it utilizes a linear perturbation from a curve for purely sinousoidal oscillations. It was shown by Fonda[12] that this relationship could be derived by using an equation equivalent to (9) to perturb around the U-g curve. The second, more complicated method needs only to be used for charting eigenvalues for speeds beyond that for class C instability. Comparisons with a limited amount of exact calculations show these methods to be

highly successful, at least for simple systems. Once the characteristic curve has been obtained, the eigenvalues are easily estimated from simple slide-rule calculations involving distances measured in the characteristic diagram by a ruler. Thus, for the first time, a simple and yet rather accurate technique is provided whereby approximate values of actual complex eigenvalues may be obtained from aerodynamic forces evaluated for purely oscillatory motion. Since the way the characteristic equation is obtained is immaterial, the graphical technique could also be used, for example, to estimate eigenvalues from measurements of the complex impedance in some point of the system. Such a procedure could possibly be used with advantage for flight flutter tests, since the possibility of violent class C instability could then be detected from the shape of the impedance curve for velocities well below that of flutter.

The main shortcoming of the present method is for cases where three or more nearly real eigenvalues are located close together. However, in contrast to the merging of two roots, which is believed to be typical of systems with flowing fluids, the limited experience so far indicates that clustering of three or more eigenvalues is fairly rare. For systems with high mass-density ratios, as in wing flutter, this would primarily occur when the natural (uncoupled) frequencies of the system are close together. As is well known to aeroelasticians, however, this is a condition to be avoided, lest severe instability be invited.

The second shortcoming of the method is that it will not work for eigenvalues that are located far from the real axis, and the possibility thus exists that a severe instability may remain undetected. However, systems with fluid flow must always be stable for sufficiently low velocities, and it should therefore in practice always be possible to trace an instability from the velocity at which it first becomes marginally unstable using the present technique.

References

[1] Zisfein, M. B. and Frueh, F. J., "A study of velocity-frequency damping relationships for wing and panel binary systems in high-supersonic flow," Air Force Office of Scientific Research, AFOSR TN 59-969 (October 1959).

[2] Zisfein, M. B. and Frueh, F. J., "Approximation methods for aeroelastic systems in high supersonic flow," Air Force Office of Scientific Research, AFOSR TR 60-182 (October 1960).

[3] Frueh, F. J. and Zisfein, M. B., "Numerical approximation method for flexible flight vehicle transfer function factors," Aeronautical Systems Division ASD TDR 62-1063 (March 1963).

[4] Dugundji, J., "A Nyquist approach to flutter," J. Aeronaut. Sci. **19**, 442–423 (1952).

[5] Landahl, M. T., "On the stability of a laminar boundary layer over a flexible surface," J. Fluid Mech. **13**, Part 4, 609–632 (1962).

[6] Benjamin, T. B., "Effects of a flexible boundary on hydrodynamic stability," J. Fluid Mech. **9**, Part 4, 513–532 (1960).

[7] Benjamin, T. B., "The three-fold classification of unstable disturbances in flexible surfaces bounding inviscid flows," J. Fluid Mech. **16**, Part 3, 436–452 (1963).

[8] Greenspan, H. and Benney, D., "Free shear layer instability, breakdown and transition," J. Fluid Mech. **15**, Part 1, 133–153 (1963).

[9] Weatherill, W. H. and Zartarian, G., "Tabular presentation of supersonic flutter trends from piston theory calculations," Wright Air Development Center TN 57-310 (1958).

[10] Bisplinghoff, R., Ashley, H., and Halfman, R., *Aeroelasticity* (Addison-Wesley Publishing Co., Inc., Reading, Mass., 1955).

[11] Zartarian, G., Heller, A., and Ashley, H., "Application of piston theory of certain elementary aeroelastic problems," Proceedings of Second Midwestern Conference on Solid Mechanics and the Fourth Midwestern Conference on Fluid Mechanics, Purdue Univ. (September 1955).

[12] Fonda, A. G., "Decay-damping relationships for highly-coupled systems with many degrees of freedom," Air Force Office of Scientific Research, AFOSR 1317 (August 1961).